

Candidate for a passively-protected quantum memory in two dimensions

Simon Lieu^{†, 1, 2} Yu-Jie Liu^{†, 3, 4} and Alexey V. Gorshkov^{1, 2}

¹*Joint Quantum Institute, NIST/University of Maryland, College Park, Maryland 20742, USA*

²*Joint Center for Quantum Information and Computer Science,*

NIST/University of Maryland, College Park, Maryland 20742 USA

³*Department of Physics, Technical University of Munich, 85748 Garching, Germany*

⁴*Munich Center for Quantum Science and Technology (MCQST), Schellingstr. 4, 80799 München, Germany*

(Dated: July 19, 2022)

An interesting problem in the field of quantum error correction involves finding a physical system that hosts a “passively-protected quantum memory,” defined as an encoded qubit coupled to an environment that naturally wants to correct errors. To date, a quantum memory stable against finite-temperature effects is only known in four spatial dimensions or higher. Here, we take a different approach to realize a stable quantum memory by relying on a driven-dissipative environment. We propose a new model which appears to passively correct against both bit-flip and phase-flip errors in two dimensions: A square lattice composed of photonic “cat qubits” coupled via dissipative terms which tend to fix errors locally. Inspired by the presence of two distinct \mathbb{Z}_2 -symmetry-broken phases, our scheme relies on Ising-like dissipators to protect against bit flips and on a driven-dissipative photonic environment to protect against phase flips.

Quantum error correction remains one of the biggest challenges towards building a practical quantum computer [1, 2]. One of the leading candidates for realizing fault tolerance is the family of quantum stabilizer codes [3], including the surface code [4–6] and the GKP code [7]. These error-correcting schemes are based on fast error recovery controlled by the feedback from repetitive syndrome measurements.

A prominent alternative is the finite-temperature quantum memory: Certain thermal environments naturally evolve arbitrary initial states into a qubit subspace of interest at low temperature, thus eliminating the need for active measurements and correcting operations. Many recent studies have investigated thermal self-correcting properties [6, 8–19]. To date, the only known models that host a passive quantum memory via this mechanism are topological codes in four dimensions (4D) and higher, e.g. the 4D toric code [6, 19].

A separate line of research aims to uncover a passively-protected quantum memory via engineered “driven-dissipative” systems [20–39]. Such passive protection includes but is not limited to the finite-temperature case, since a thermal-equilibrium steady state is not required. The quantum memory is dynamically protected against certain noise channels by (local) Markovian dissipation. In this work, we study a model with engineered dissipation which appears to protect against both bit flips and phase flips and lives in two spatial dimensions. Instead of relying on topological order, we suggest that the model should belong to a phase that spontaneously breaks two different \mathbb{Z}_2 symmetries. Each \mathbb{Z}_2 -symmetry-broken phase protects a “classical bit,” which together

form a robust qubit.

Quantum memory.—Consider a Hilbert space \mathcal{H} , and define two encoded, logical states $|\bar{0}\rangle, |\bar{1}\rangle \in \mathcal{H}$ that span the codespace \mathcal{C} . We assume the system is always initialized in the codespace: $\rho_i = |\psi\rangle\langle\psi|$ where $|\psi\rangle \in \mathcal{C}$.

A local continuous-time Markovian generator \mathcal{L} in Lindblad form is defined by

$$\frac{d\rho}{dt} = \mathcal{L}(\rho) = -i[H, \rho] + \sum_j \left(L_j \rho L_j^\dagger - \frac{1}{2} \{L_j^\dagger L_j, \rho\} \right), \quad (1)$$

where H is the Hamiltonian of the system and L_j are local dissipators which arise due to the system-environment coupling [40]. We consider a dynamical process that can be decomposed into two parts, an “error” generator and a “recovery” generator: $\mathcal{L} = \mathcal{L}_e + \mathcal{L}_r$. The error generator describes the main channels of physical noise which move the initial state out of the codespace. The recovery generator stabilizes the codespace: $\mathcal{L}_r(\rho_i) = 0$, i.e. any state in the codespace is a steady state of the recovery. We allow for this noisy process to occur for a time t , which generically sends ρ_i to a mixed state $\rho_m(t) = e^{\mathcal{L}t}(\rho_i)$.

Finally, we employ a “single-shot” decoding quantum channel \mathcal{E}_r which sends every state in the Hilbert space back to the codespace [41]. The final state is

$$\rho_f(t) = \mathcal{E}_r e^{\mathcal{L}t}(\rho_i). \quad (2)$$

We wish to find systems where the difference between the initial and final states is exponentially small in the system size:

$$1 - \text{Tr}[\rho_i \rho_f(t)] = O(e^{-\gamma M}) \text{ as } M \rightarrow \infty, \quad (3)$$

where $\gamma > 0$ is a time-independent constant and M is the linear system size. A system described by \mathcal{L} hosts a

[†] These authors contributed equally.

passively-protected quantum memory for any finite time t if Eq. (3) holds as the thermodynamic limit is approached: The recovery Lindbladian \mathcal{L}_r ensures that errors do not corrupt quantum information for any finite time.

The bit-flip and phase-flip errors of a two-level system are generated via the Pauli operators X, Z respectively. A good quantum memory should thus protect against both sources of noise. Recent work [39] has described the connection between \mathbb{Z}_2 symmetry breaking and error correction: A symmetry-broken phase protects quantum information against X or Z errors, but not both. This leads to a protected classical bit, which can be viewed as a quantum bit experiencing biased noise [42].

In this work, we attempt to glue two different classical bits together to form a robust qubit. Our strategy involves studying a system that passively corrects against bit flips due to Ising-like dissipators which tend to align qubits locally. Furthermore, phase flips will passively correct due to driven-dissipative stabilization of the photonic cat code. We begin by describing spontaneous symmetry breaking in the cat code and in the Ising model separately. We then describe a model which inherits both protecting features.

Photonic cat code.—Let us briefly review \mathbb{Z}_2 spontaneous symmetry breaking in the photonic cat code [28, 43]. [For a detailed analysis, we refer to Ref. [39].] Consider a driven-dissipative photonic cavity in the presence of two-photon drive and two-photon loss. The rotating-frame Hamiltonian and dissipator read $H = \lambda(a^2 + (a^\dagger)^2)$, $L_2 = \sqrt{\kappa_2}a^2$. Here a is the annihilation operator for a cavity photon, λ is the drive strength, and κ_2 is the two-photon loss rate. While the model has \mathbb{Z}_2 symmetry $[H, Q] = [L_2, Q] = 0$ generated by parity $Q = e^{i\pi a^\dagger a}$, the steady state can violate this symmetry:

$$\rho_{ss} = |\psi\rangle\langle\psi|, \quad |\psi\rangle = c_0|\alpha_e\rangle + c_1|\alpha_o\rangle, \quad (4)$$

for $|c_0|^2 + |c_1|^2 = 1$, where $|\alpha_e\rangle \sim |\alpha\rangle + |-\alpha\rangle$, $|\alpha_o\rangle \sim |\alpha\rangle - |-\alpha\rangle$, and $|\alpha\rangle$ is a coherent state with amplitude $\alpha = e^{-i\pi/4}\sqrt{N}$ and $N \equiv \lambda/\kappa_2$ photons. The even and odd cat states $|\alpha_{e/o}\rangle$ represent logical 0 and 1, respectively.

The cat code is protected against phase-flip errors generated by photon dephasing $L_d = \sqrt{\kappa_d}a^\dagger a$. Indeed, the phase-flip logical error rate scales as $e^{-\gamma N}$ where γ is a constant [28]. The symmetry-broken states $|\pm\alpha\rangle \approx (|\alpha_e\rangle \pm |\alpha_o\rangle)/\sqrt{2}$ have an exponentially-long lifetime in the limit of large N , ensuring that logical phase flips are unlikely.

The dominant decoherence mechanism for the cat qubit stems from the bit flip, generated via single-photon loss $L_1 = \sqrt{\kappa_1}a$: $a|\alpha_{e/o}\rangle \sim |\alpha_{o/e}\rangle$, which reduces the qubit steady state structure to a classical bit: $\rho_{ss} \approx c|+\alpha\rangle\langle+\alpha| + (1-c)|-\alpha\rangle\langle-\alpha|$, $c \in [0, 1]$ [39]. More generally, perturbations that commute with photon parity (e.g. $[L_d, Q] = 0$) are expected to be passively cor-

rected, while terms which explicitly break the symmetry (e.g. $\{L_1, Q\} = 0$) are not.

2D Ising model.—We now turn our attention to a system that has the opposite problem: \mathbb{Z}_2 symmetry breaking will protect against bit flips but not phase flips. In particular, we construct local dissipators which reproduce the thermal phase transition for the 2D classical Ising model. The low-temperature phase protects a classical bit against bit flips.

We design a local Lindbladian such that its steady state is the thermal state of the 2D Ising model on an $M \times M$ lattice with periodic boundary conditions. The 2D Ising model Hamiltonian reads

$$H_{is} = - \sum_{x,y=1}^M (Z_{x,y}Z_{x+1,y} + Z_{x,y}Z_{x,y+1}), \quad (5)$$

where $Z_{x,y}$ is the Z Pauli operator on site (x, y) . The ferromagnetic states are the ground states of this model and span the codespace: $|\bar{0}\rangle \equiv |\downarrow\downarrow\ldots\rangle$, $|\bar{1}\rangle \equiv |\uparrow\uparrow\ldots\rangle$, with $Z|\downarrow\rangle = |\downarrow\rangle$ and $Z|\uparrow\rangle = -|\uparrow\rangle$.

We define dissipators and bit flips that locally obey detailed balance with respect to this Hamiltonian. (For simplicity, we set the Hamiltonian in the master equation to zero.) Consider dissipators that are a product of a spin flip (X) with a projector onto a particular domain-wall configuration. In other words, these jumps will cause a spin to flip sign according to a local “majority rule,” i.e. only if more than two of the neighboring spins are misaligned. Specifically:

$$\begin{aligned} L_{x,y}^{(4)} &= \sqrt{\kappa}X_{x,y}P_{x,y;\rightarrow}^-P_{x,y;\uparrow}^-P_{x-1,y;\rightarrow}^-P_{x,y-1;\uparrow}^-, \\ L_{x,y}^{(3)} &= \sqrt{\tilde{\kappa}}X_{x,y}P_{x,y;\rightarrow}^+P_{x,y;\uparrow}^-P_{x-1,y;\rightarrow}^-P_{x,y-1;\uparrow}^-, \end{aligned} \quad (6)$$

where $\tilde{\kappa} = \sqrt{\Delta\kappa + \Delta^2} - \Delta$ and $P_{x,y;\rightarrow}^\pm = (1 \pm Z_{x,y}Z_{x+1,y})/2$, $P_{x,y;\uparrow}^\pm = (1 \pm Z_{x,y}Z_{x,y+1})/2$ are projectors onto particular local configurations of spins. The superscripts indicate the number of domain walls which the projector is checking for, and we neglect to write jumps related by rotational invariance (i.e. there are 4 different $L^{(3)}$ operators per site) [44]. We also consider an error process in the form of a uniform bit flip rate on each lattice site:

$$L'_{x,y} = \sqrt{\Delta}X_{x,y}. \quad (7)$$

We have chosen our dissipators above such that the steady state of the model is the thermal state of the 2D classical Ising model:

$$\rho_{ss} = \frac{e^{-\beta H_{is}}}{\text{Tr}[e^{-\beta H_{is}}]}, \quad \beta = \frac{1}{8} \ln \left[\frac{\kappa + \Delta}{\Delta} \right], \quad (8)$$

with the effective temperature set by the relative ratio of the correction rate to the bit-flip rate. Within the quantum jump picture [45, 46], the rates of transitioning

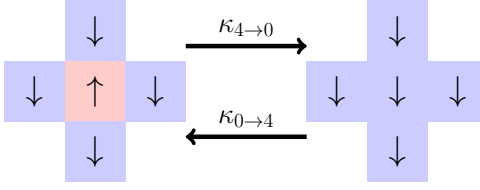


FIG. 1. The total rate of transitioning from a configuration with 4 domain walls to a configuration with 0 domain walls satisfies detailed balance: $\kappa_{4\rightarrow 0}/\kappa_{0\rightarrow 4} = e^{8\beta}$.

between different classical configurations respect detailed balance. (See e.g. Fig. 1.)

While the thermal state (8) is always a steady state of the model, it is not unique. All dissipators commute with the parity operator $Q = \prod_{i=1}^{M^2} X_i$: $[L_j, Q] = 0$, which means that the dynamics preserves the parity of the state (called a “strong \mathbb{Z}_2 symmetry” [47]). This implies that there are at least two different steady states, one for each parity sector. However this degeneracy is enlarged to four in the symmetry-broken phase. In the thermodynamic limit of the low-temperature phase, the steady state is:

$$\rho_{ss} = \sum_i \frac{e^{-\beta E_i}}{Z} (|E_i^+\rangle, |E_i^-\rangle) \begin{pmatrix} |c_0|^2 & c_0 c_1 \\ c_0^* c_1^* & |c_1|^2 \end{pmatrix} \begin{pmatrix} \langle E_i^+ | \\ \langle E_i^- | \end{pmatrix}, \quad (9)$$

for $|c_0|^2 + |c_1|^2 = 1$, where the states $|E_i^\pm\rangle$ are energy eigenstates of the classical Ising Hamiltonian labeled by their parity: $Q|E_i^\pm\rangle = \pm|E_i^\pm\rangle$. This is an example of a “noiseless subsystem,” and implies that a qubit can be stored in the steady state [48–50].

We can confirm this picture via numerical simulations. Suppose we initialize our system in a ferromagnetic state: $|\psi\rangle = |\bar{0}\rangle = (|E_0^+\rangle + |E_0^-\rangle)/\sqrt{2}$ where $|E_0^\pm\rangle$ are ground states in the different parity sectors [51]. We then quench the system with the noisy Lindbladian for a time T much larger than the inverse of the dissipative gap, so that the system settles into its steady state. Finally, we apply a single-shot decoder which brings the state back to the codespace by measuring all domain walls in the system then flipping all bits in the smaller domain.

Our results are summarized in Fig. 2. In the low-temperature phase, the overlap starts to approach the ideal value of 1 exponentially fast in M . Qualitatively different behavior occurs in the high-temperature phase [$\beta > \beta_c = \ln(1 + \sqrt{2})/2 \approx 0.44$; red dots], where the success rate of the decoder is only 50%.

Unfortunately, such a qubit structure (9) is unstable to noise that violates the strong symmetry. In particular, the presence of Z dephasing (phase flips), $L_i \sim Z_i$, reduces the strong \mathbb{Z}_2 symmetry to a “weak \mathbb{Z}_2 symmetry” (defined at the level of the superoperator: $[\mathcal{L}, \mathcal{Q}] = 0$, where $\mathcal{Q}(\rho) = Q\rho Q^\dagger$), such that only a classical bit can be stored in the steady state. In this

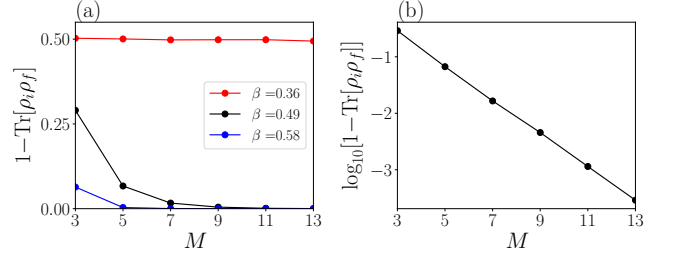


FIG. 2. (a) The overlap between the initial and final states for the protocol given in the main text, for a Lindbladian in the high-temperature phase (red dots), and in the low-temperature phase (black and blue dots). As linear system size M grows, the overlap approaches one only in the low-temperature (symmetry-broken) phase corresponding to $\beta > \beta_c \approx 0.44$. (b) Same black data points on a log plot; the overlap tends to one exponentially fast in M . In both (a) and (b), the quench time is $T = 800/\kappa$, i.e. long enough to reach the steady state. The simulation employs the quantum jump approach by averaging over 10^5 trajectories.

case, the steady state at low-temperature has the structure $\rho_{ss} \approx c|\bar{0}\rangle\langle\bar{0}| + (1-c)|\bar{1}\rangle\langle\bar{1}|$, for $c \in [0, 1]$. In analogy with the cat qubit in the presence of single-photon loss, Z dephasing destroys the coherence between Ising ferromagnetic states.

2D photonic-Ising model.—We have found that the cat code passively corrects against phase flips but not bit flips, and that the 2D Ising model passively corrects against bit flips but not phase flips. Is it possible to combine the protecting features of both models to construct a system that passively corrects against both sources of noise?

Consider an $M \times M$ square lattice of photonic cavities. Each cavity undergoes a two-photon drive process and a two-photon loss process:

$$H_{x,y} = \lambda(a_{x,y}^2 + (a_{x,y}^\dagger)^2), \quad L_{2,x,y} = \sqrt{\kappa_2}a_{x,y}^2, \quad (10)$$

where $a_{x,y}$ is the annihilation operator on site (x, y) . Next, we consider local nearest-neighbor dissipators of the following form:

$$\begin{aligned} L_{x,y}^{(4)} &= \sqrt{\kappa_{nn}}a_{x,y}P_{x,y;\rightarrow}^-P_{x,y;\uparrow}^-P_{x-1,y;\rightarrow}^-P_{x,y-1;\uparrow}^-, \\ L_{x,y}^{(3)} &= \sqrt{\tilde{\kappa}_{nn}}a_{x,y}P_{x,y;\rightarrow}^+P_{x,y;\uparrow}^-P_{x-1,y;\rightarrow}^-P_{x,y-1;\uparrow}^-, \end{aligned} \quad (11)$$

where $a_{x,y}$ is the annihilation operator for the cavity at site x, y , $\tilde{\kappa}_{nn} = \sqrt{\kappa_1\kappa_{nn} + \kappa_1^2} - \kappa_1$, κ_1 is the single-photon loss rate (corresponding to the dissipator: $L_{1,x,y} = \sqrt{\kappa_1}a_{x,y}$), $P_{x,y;\rightarrow}^\pm = (1 \pm Q_{x,y}Q_{x+1,y})/2$, $P_{x,y;\uparrow}^\pm = (1 \pm Q_{x,y}Q_{x,y+1})/2$, and $Q_{x,y} = e^{i\pi a_{x,y}^\dagger a_{x,y}}$. The following states are the steady states of the model in the absence of errors ($\kappa_1 = 0$) and span the codespace:

$$|\psi\rangle = c_0|\alpha_e\rangle|\alpha_e\rangle|\alpha_e\rangle \dots + c_1|\alpha_o\rangle|\alpha_o\rangle|\alpha_o\rangle \dots, \quad (12)$$

for $|c_0|^2 + |c_1|^2 = 1$.

For thermal systems, the existence of a passively-correcting quantum memory is related to the presence of an extensive energy barrier which local errors must overcome in order to create a logical bit-flip or phase-flip operation [52]. In the model described above, a logical bit-flip operation can be created via local single-photon loss $L_{1,x,y} = \sqrt{\kappa_1}a_{x,y}$ only by passing through a configuration with an extensive number of domain walls, which is exponentially unlikely in the limit of large lattice size $M \rightarrow \infty$. Similarly, a phase-flip error can only be generated by taking the state $|\alpha_e\rangle \pm |\alpha_o\rangle$ to $|\alpha_e\rangle \mp |\alpha_o\rangle$ for any of the cavities. However, such a process is also unlikely to occur via dephasing perturbations $L_{d,x,y} = \sqrt{\kappa_d}a_{x,y}^\dagger a_{x,y}$ which perturb states locally in phase space, since the states $|\pm\alpha\rangle \approx |\alpha_e\rangle \pm |\alpha_o\rangle$ are well separated in phase space and an unstable fixed point sits between them [53]. The logical phase-flip errors are again exponentially unlikely as $N \rightarrow \infty$.

The single-photon loss and the dephasing lead to terms proportional to $a^\dagger a$ and $(a^\dagger a)^2$ in the Lindbladian, which result in leakage out of the effective two-level codespace for each cavity into other states of the cavity. This leakage poses a challenge for numerical simulation since (unlike the Ising model) we need to keep track of more than two degrees of freedom per lattice site. Nevertheless, we shall provide evidence for a stable quantum memory by employing a variety of approximations.

First, let us consider an approximation that allows us to map the dynamics of the photonic-Ising model directly to the classical-Ising model studied above. Specifically, we introduce an idealized model by replacing the single-photon loss dissipator $L_1 = \sqrt{\kappa_1}a$ with $E_1 = \sqrt{\kappa_1}b$, where $b = aV$ and V is the projector onto the codespace: $V = |\alpha_e\rangle\langle\alpha_e| + |\alpha_o\rangle\langle\alpha_o|$. We also assume an absence of dephasing errors, i.e. $\kappa_d = 0$. This allows us to treat each site as an effective two-level system $|0\rangle = |\alpha_e\rangle, |1\rangle = |\alpha_o\rangle$, avoiding any leakage out of the codespace. We similarly replace $a \rightarrow b$ in the nearest-neighbor coupling dissipators (11) (except in the definition of Q). The operator b can be regarded as an ‘‘idealized bit flip’’ since, for $N \gg 1$, it takes the form $b \approx \alpha(|\alpha_e\rangle\langle\alpha_o| + |\alpha_o\rangle\langle\alpha_e|)$. The idealized model maps exactly to the Ising model studied above, with an effective bit-flip error rate of $N\kappa_1$, an effective Ising-correction rate of $N\kappa_{nn}$, and an inverse temperature $\beta = \ln[(\kappa_{nn} + \kappa_1)/\kappa_1]/8$. We therefore find that this model passively corrects against bit flips in the limit $M \rightarrow \infty$ of the low-temperature phase. In the limit of large driving strength and small single-photon loss, we expect the photonic-Ising model to be well approximated by the idealized model since the state rarely leaves the codespace. We provide quantitative evidence for this in the Supplemental Material (SM) [54].

Dephasing, single-photon loss, and bit-flip recovery jumps ($L_{x,y}^{(3)}$ and $L_{x,y}^{(4)}$) cause leakage out of the codespace which is neglected within the idealized model. It is natural to ask whether this leakage is detrimental to the

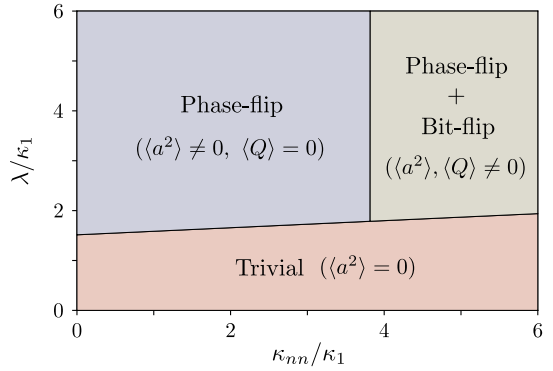


FIG. 3. The mean-field phase diagram for $\kappa_d = \kappa_1$. The top right corner shades the region where both $\langle Q \rangle$ and $\langle a^2 \rangle$ are non-zero. Both phase and bit-flip errors are protected. When $\langle a^2 \rangle \neq 0$ but $\langle Q \rangle = 0$, we expect protection only for phase errors. When $\langle a^2 \rangle = 0$, we expect the memory to become fragile under either noise.

passively-protected memory when the idealized model is no longer a good approximation. We provide evidence that this is not the case by studying a toy model which resembles the 2D model. Consider a single cavity coupled to a spin-1/2 particle (described by Pauli operators X, Y, Z), leading to two logical states $|\downarrow\rangle|\alpha_e\rangle$ and $|\downarrow\rangle|\alpha_o\rangle$. The Hamiltonian and jump operators read $h = \lambda(a^2 + (a^\dagger)^2)$, $l_2 = \sqrt{\kappa_2}a^2$, $l_1 = \sqrt{\kappa_1}Xa$, $l_d = \sqrt{\kappa_d}a^\dagger a$, $l_{nn} = \sqrt{\kappa_{nn}}\frac{1}{2}X(1-Z)a$. The model assumes that single-photon loss is accompanied by a spin flip, while two-photon drive and dephasing are not. The flip-recovery jump l_{nn} is triggered by a flipped spin state $|\uparrow\rangle$, similar to the bit-flip recovery jump caused by a parity misalignment in 2D. Importantly, leakage caused by the noise processes l_1, l_d , and the flip-recovery jump is captured by this model. In the SM [54], we analyze this model numerically and analytically. We find that the initial state can always be perfectly restored via a decoder (up to corrections exponentially small in N).

Finally, the stability of the memory can also be understood as the coexistence of two order parameters: $\langle Q \rangle = \langle e^{i\pi a^\dagger a} \rangle \neq 0$ indicates the ferromagnetic phase and therefore suppression of bit-flip errors, while $\langle a^2 \rangle \neq 0$ indicates that the cat states are stabilized, implying suppression of phase-flip errors. We use a product-state mean-field ansatz $\rho = \bigotimes_{x,y=1}^M \rho_{x,y}$, where each $\rho_{x,y}$ is a density matrix for a two-level system in the basis of $|\pm\alpha_{MF}\rangle$ for some mean-field coherent parameter α_{MF} . A non-trivial ordering of the system is identified by non-zero fixed points of $\langle Q \rangle$ and $\langle a^2 \rangle$. The mean-field solutions suggest that, for small κ_1, κ_d , both phase and bit-flip errors are exponentially suppressed. When κ_1 or κ_d exceeds a threshold, the order parameters undergo two second-order phase transitions and the quantum memory is no longer stable (see the SM [54]). The mean-field phase diagram is sketched in Fig. 3.

Discussion and outlook.—Photonic cat qubits are the building blocks for several proposals aimed at achieving a fault-tolerant quantum computer [42, 53]. A promising solution for dealing with the bit-flip error in the cat code is to construct a quantum repetition code using cat codes on a 1D lattice. The bit-flip errors are detected and recovered globally by repeated fast syndrome measurements [42, 53]. In contrast to this active protocol, our result suggests that the errors can be continuously suppressed by local interactions in 2D.

We can estimate the logical error rates in the photonic-Ising model as follows. While the bit-flip error rate becomes extensive ($\sim O(N)$) in the limit of large cavity photon number, the Ising-type interaction gives rise to an exponentially-suppressed error rate $O(\text{poly}(M)e^{-\gamma M})$ with $\gamma > 0$ [55–57], resulting in a logical bit-flip error rate of $O(N\text{poly}(M)e^{-\gamma M})$. Similarly, a single cavity yields a phase-flip error rate of $O(e^{-\gamma' N})$ with $\gamma' > 0$, while this is made extensive by the spatially-extended lattice configuration, resulting in a logical phase flip error rate of $O(M^2 e^{-\gamma' N})$. Harmonic oscillators with small non-linearities and outstanding coherence properties—and thus with large achievable N —can be found in a variety of photonic and phononic systems (e.g. [38, 58]).

The key ingredients for our proposal are the nearest-neighbor coupling dissipators defined in Eq. (11). Future efforts should design schemes that realize such effective dissipators in experiments. We note that dissipators of the form: $L \sim a^\dagger P$ (where P is a projector onto a parity state) have been proposed theoretically [59, 60] and realized experimentally [61] in the context of fixing errors from single-photon loss for a single cavity. We speculate that similar techniques can be used for many-body generalizations. The coupling dissipators (11) also arise naturally as the thermal dissipators for the Ising-like Hamiltonian $H = -\sum_{\langle ij \rangle} Q_i Q_j$, where Q_i is the photon parity operator for cavity i , and j is its nearest neighbor. Schemes that result in the Hamiltonian terms $Q_i Q_j$ have been proposed [59, 60]. The dissipators (11) could also be implemented digitally with the assistance of ancilla qubits, similar to the setup in Ref. [62]. A single time step is implemented by storing the result of a $Q_i Q_j$ measurement [42, 53, 60] in an ancilla, applying a gate on it, and then using an incoherent process to reset the ancilla.

The photonic-Ising model can be generalized to adapt the Toom’s rule [63], or to higher dimensions [64] for a better tolerance against single-photon loss and a more robust perturbative stability. The full perturbative stability of the model remains an interesting open question.

Acknowledgment.—We sincerely thank Oles Shtanko, Victor Albert, and Daniel Slichter for useful discussions. We thank Fernando Brandão for pointing out Ref. [64] regarding the perturbative stability of a three-dimensional model. S.L. was supported by the NIST NRC Research Postdoctoral Associateship. Y.-J.L was supported by the Max Planck Gesellschaft (MPG) through the Interna-

tional Max Planck Research School for Quantum Science and Technology (IMPRS-QST). A.V.G. acknowledges funding by NSF QLCI (award No. OMA-2120757), DoE QSA, DoE ASCR Accelerated Research in Quantum Computing program (award No. DE-SC0020312), ARO MURI, AFOSR, DARPA SAVaNT ADVENT, DoE ASCR Quantum Testbed Pathfinder program (award No. DE-SC0019040), U.S. Department of Energy Award No. DE-SC0019449, NSF PFCQC program, and AFOSR MURI.

- [1] M. A. Nielsen and I. Chuang, *Quantum computation and quantum information* (American Association of Physics Teachers, 2002).
- [2] D. A. Lidar and T. A. Brun, *Quantum error correction* (Cambridge university press, 2013).
- [3] D. Gottesman, *Stabilizer codes and quantum error correction*, Ph.D. thesis, California Institute of Technology (1997).
- [4] S. B. Bravyi and A. Y. Kitaev, [arXiv preprint quant-ph/9811052](https://arxiv.org/abs/quant-ph/9811052) (1998).
- [5] A. G. Fowler, M. Mariantoni, J. M. Martinis, and A. N. Cleland, *Phys. Rev. A* **86**, 032324 (2012).
- [6] E. Dennis, A. Kitaev, A. Landahl, and J. Preskill, *J. Math. Phys.* **43**, 4452 (2002).
- [7] D. Gottesman, A. Kitaev, and J. Preskill, *Phys. Rev. A* **64**, 012310 (2001).
- [8] D. Bacon, *Phys. Rev. A* **73**, 012340 (2006).
- [9] B. Yoshida, *Ann. Phys.* **326**, 2566 (2011).
- [10] S. Roberts and S. D. Bartlett, *Phys. Rev. X* **10**, 031041 (2020).
- [11] B. M. Terhal, *Rev. Mod. Phys.* **87**, 307 (2015).
- [12] B. J. Brown, D. Loss, J. K. Pachos, C. N. Self, and J. R. Woottton, *Rev. Mod. Phys.* **88**, 045005 (2016).
- [13] H. Bombin, R. W. Chhajlany, M. Horodecki, and M. A. Martin-Delgado, *New J. Phys.* **15**, 055023 (2013).
- [14] J. Haah, *Phys. Rev. A* **83**, 042330 (2011).
- [15] S. Bravyi and J. Haah, *Phys. Rev. Lett.* **111**, 200501 (2013).
- [16] S. Chesi, B. Röthlisberger, and D. Loss, *Phys. Rev. A* **82**, 022305 (2010).
- [17] N. P. Breuckmann, K. Duivenvoorden, D. Michels, and B. M. Terhal, [arXiv preprint arXiv:1609.00510](https://arxiv.org/abs/1609.00510) (2016).
- [18] R. Alicki, M. Fannes, and M. Horodecki, *J. Phys. A: Math. Theor.* **42**, 065303 (2009).
- [19] R. Alicki, M. Horodecki, P. Horodecki, and R. Horodecki, *Open Sys. Inf. Dyn.* **17**, 1 (2010).
- [20] J. P. Paz and W. H. Zurek, *Proc. R. Soc. A: Math. Phys. Eng. Sci.* **454**, 355 (1998).
- [21] J. P. Barnes and W. S. Warren, *Phys. Rev. Lett.* **85**, 856 (2000).
- [22] C. Ahn, A. C. Doherty, and A. J. Landahl, *Phys. Rev. A* **65**, 042301 (2002).
- [23] M. Sarovar and G. J. Milburn, *Phys. Rev. A* **72**, 012306 (2005).
- [24] O. Oreshkov and T. A. Brun, *Phys. Rev. A* **76**, 022318 (2007).
- [25] J. Kerckhoff, H. I. Nurdin, D. S. Pavlichin, and H. Mabuchi, *Phys. Rev. Lett.* **105**, 040502 (2010).

[26] J.-M. Lihm, K. Noh, and U. R. Fischer, *Phys. Rev. A* **98**, 012317 (2018).

[27] F. Pastawski, L. Clemente, and J. I. Cirac, *Phys. Rev. A* **83**, 012304 (2011).

[28] M. Mirrahimi, Z. Leghtas, V. V. Albert, S. Touzard, R. J. Schoelkopf, L. Jiang, and M. H. Devoret, *New J. Phys.* **16**, 045014 (2014).

[29] E. Kapit, *Phys. Rev. Lett.* **116**, 150501 (2016).

[30] F. Reiter, A. S. Sørensen, P. Zoller, and C. A. Muschik, *Nat. Commun.* **8**, 1822 (2017).

[31] K. Fujii, M. Negoro, N. Imoto, and M. Kitagawa, *Phys. Rev. X* **4**, 041039 (2014).

[32] N. Ofek, A. Petrenko, R. Heeres, P. Reinhold, Z. Leghtas, B. Vlastakis, Y. Liu, L. Frunzio, S. M. Girvin, L. Jiang, M. Mirrahimi, M. H. Devoret, and R. J. Schoelkopf, *Nature* **536**, 441 (2016).

[33] A. Gyenis, P. S. Mundada, A. Di Paolo, T. M. Hazard, X. You, D. I. Schuster, J. Koch, A. Blais, and A. A. Houck, *PRX Quantum* **2**, 010339 (2021).

[34] P. Campagne-Ibarcq, A. Eickbusch, S. Touzard, E. Zalys-Geller, N. E. Frattini, V. V. Sivak, P. Reinhold, S. Puri, S. Shankar, R. J. Schoelkopf, L. Frunzio, M. Mirrahimi, and M. H. Devoret, *Nature* **584**, 368 (2020).

[35] Z. Leghtas, S. Touzard, I. M. Pop, A. Kou, B. Vlastakis, A. Petrenko, K. M. Sliwa, A. Narla, S. Shankar, M. J. Hatridge, *et al.*, *Science* **347**, 853 (2015).

[36] R. W. Heeres, P. Reinhold, N. Ofek, L. Frunzio, L. Jiang, M. H. Devoret, and R. J. Schoelkopf, *Nat. Commun.* **8**, 94 (2017).

[37] R. Lescanne, M. Villiers, T. Peronni, A. Sarlette, M. Delbecq, B. Huard, T. Kontos, M. Mirrahimi, and Z. Leghtas, *Nat. Phys.* **16**, 509 (2020).

[38] C. Berdou, A. Murani, U. Reglade, W. Smith, M. Villiers, J. Palomo, M. Rosticher, A. Denis, P. Morfin, M. Delbecq, *et al.*, *arXiv preprint arXiv:2204.09128* (2022).

[39] S. Lieu, R. Belyansky, J. T. Young, R. Lundgren, V. V. Albert, and A. V. Gorshkov, *Phys. Rev. Lett.* **125**, 240405 (2020).

[40] G. Lindblad, *Commun. Math. Phys.* **48**, 119 (1976).

[41] If the code space spans the kernel of \mathcal{L}_r , then a natural choice for the decoder is $\mathcal{E}_r = \lim_{t \rightarrow \infty} e^{\mathcal{L}_r t}$. Such a decoder is typically used for the cat code. However, if \mathcal{L}_r has other steady states which are not in the code space, such a decoder is not ideal. We do not use this decoder for the Ising model, since its \mathcal{L}_r has steady states outside of the code space.

[42] C. Chamberland, K. Noh, P. Arrangoiz-Arriola, E. T. Campbell, C. T. Hann, J. Iverson, H. Puttermann, T. C. Bohdanowicz, S. T. Flammia, A. Keller, G. Refael, J. Preskill, L. Jiang, A. H. Safavi-Naeini, O. Painter, and F. G. Brandão, *PRX Quantum* **3**, 010329 (2022).

[43] L. Gilles, B. M. Garraway, and P. L. Knight, *Phys. Rev. A* **49**, 2785 (1994).

[44] We could also include jumps that flip a spin if there are two domain walls surrounding it, e.g. $L^{(2)} = \sqrt{\gamma} X_{x,y} P_{x,y; \rightarrow}^+ P_{x,y; \uparrow}^+ P_{x-1,y; \rightarrow}^- P_{x,y-1; \uparrow}^-$, since such a process does not change the energy and hence respects detailed balance (for any rate γ). Consequently, such jumps do not change the exact thermal steady state solutions. We choose not to include such jumps since the mean-field solution is more accurate without them.

[45] M. B. Plenio and P. L. Knight, *Rev. Mod. Phys.* **70**, 101 (1998).

[46] A. J. Daley, *Adv. Phys.* **63**, 77 (2014).

[47] B. Buća and T. Prosen, *New J. Phys.* **14**, 073007 (2012).

[48] D. A. Lidar, I. L. Chuang, and K. B. Whaley, *Phys. Rev. Lett.* **81**, 2594 (1998).

[49] E. Knill, R. Laflamme, and L. Viola, *Phys. Rev. Lett.* **84**, 2525 (2000).

[50] V. V. Albert and L. Jiang, *Phys. Rev. A* **89**, 022118 (2014).

[51] If the symmetry-broken initial state $|\bar{0}\rangle$ is recoverable, then so is any state in the code space. This is because an arbitrary state in the code space can be expressed as: $c_0|\bar{0}\rangle + c_1|\bar{1}\rangle = (c_0 - c_1)|\bar{0}\rangle + c_1(|\bar{0}\rangle + |\bar{1}\rangle)$. Since the dynamics is linear, and the symmetric state $|\bar{0}\rangle + |\bar{1}\rangle$ can always be properly recovered in the absence of Z dephasing, this implies that any state in the code space is recoverable if $|\bar{0}\rangle$ is recoverable.

[52] S. Bravyi and B. Terhal, *New J. Phys.* **11**, 043029 (2009).

[53] J. Guillaud and M. Mirrahimi, *Phys. Rev. X* **9**, 041053 (2019).

[54] See the Supplemental Material.

[55] L. E. Thomas, *Commun. Math. Phys.* **126**, 1 (1989).

[56] R. H. Schonmann, *Commun. Math. Phys.* **112**, 409 (1987).

[57] D. Randall, in *Proceedings of the Seventeenth Annual ACM-SIAM Symposium on Discrete Algorithm*, SODA '06 (Society for Industrial and Applied Mathematics, USA, 2006) p. 870–879.

[58] J. P. Home, D. Hanneke, J. D. Jost, D. Leibfried, and D. J. Wineland, *New J. Phys.* **13**, 073026 (2011).

[59] J. Cohen, *Autonomous quantum error correction with superconducting qubits*, Ph.D. thesis, Ecole Normale Supérieure (2017).

[60] J. Cohen, W. C. Smith, M. H. Devoret, and M. Mirrahimi, *Phys. Rev. Lett.* **119**, 060503 (2017).

[61] J. M. Gertler, B. Baker, J. Li, S. Shirol, J. Koch, and C. Wang, *Nature* **590**, 243 (2021).

[62] H. Weimer, M. Müller, I. Lesanovsky, P. Zoller, and H. P. Büchler, *Nat. Phys.* **6**, 382 (2010).

[63] A. L. Toom, *Problems Inform. Transmission* **10**, 239 (1974).

[64] D. Poulin, R. G. Melko, and M. B. Hastings, *Phys. Rev. B* **99**, 094103 (2019).

Supplemental Material for “Candidate for a passively-protected quantum memory in two dimensions”

The Supplemental Material is organized as follows: In Sec. 1, we provide numerical evidence that the idealized bit flip approximation introduced in the main text is reasonable in the limit of large drive, small single-photon loss, and no dephasing. In Sec. 2, we study a “toy model”, which was introduced in the main text, which mimics the dynamics of the 2D photonic-Ising model, and which is tractable both numerically and analytically. This model suggests that leakage out of the codespace arising from single-photon loss and dephasing is not detrimental to passive correction. In Sec. 3, we provide details on the mean-field theory order parameters described in the main text.

1. IDEALIZED BIT FLIP APPROXIMATION

In this section, we elaborate on the idealized bit flip approximation used in the main text. In experiments, the bit flip error for a single photonic cat qubit is generated via single-photon loss $L_1 = \sqrt{\kappa_1}a$. However, in order to map our many-body-cat-qubit system to the 2D Ising model, we must replace this noise generator with an “idealized bit flip”, represented via the jump operator: $E_1 = \sqrt{\kappa_1}aV$ where V is a projector onto the codespace. We provide evidence that E_1 is a reasonable approximation for L_1 in the limit of small single-photon loss and large two-photon drive (compared to the two-photon loss rate), which is the relevant regime for modern experiments involving photonic cat qubits [42]. We also assume the absence of photon dephasing. To this end, we shall present two models for a single cavity and show that their steady states and dissipative gaps converge in this limit.

Model 1 has the standard single-photon loss term which is expected to appear in experiment. Model 2 has the “idealized bit flip” which is needed to make numerical progress.

Model 1: Let us consider a single photonic cavity in the presence of two-photon drive $H = \lambda[a^2 + (a^\dagger)^2]$, two photon loss $L_2 = \sqrt{\kappa_2}a^2$, and single-photon loss $L_1 = \sqrt{\kappa_1}a$. It is convenient to utilize the gauge freedom of the Lindbladian to eliminate the Hamiltonian by incorporating it in a dissipative term. The following two dissipators share the same master equation as the model just described:

$$L_c = \sqrt{\kappa_2}(a^2 - \alpha^2), \quad \alpha = \sqrt{\frac{\lambda}{\kappa_2}}e^{-i\pi/4} \quad (S1)$$

$$L_1 = \sqrt{\kappa_1}a. \quad (S2)$$

The dissipator L_c will cause states in the Hilbert space to evolve towards the coherent states $|\pm\alpha\rangle$, which are dark states of L_c . We thus find that L_c generates the “recovery” part of the Lindbladian, while L_1 generates bit flip errors and causes leakage out of the codespace.

From the perspective of quantum trajectories, single-photon loss causes the amplitude of a coherent state to decay due to the non-Hermitian Hamiltonian term proportional to $\kappa_1 a^\dagger a$ which (by itself) causes the coherent state parameter to decay via $\alpha e^{-\kappa_1 t}$. The two-photon drive process ensures that the steady state amplitude remains non-zero, but nevertheless the photon population decreases due to the single-photon loss. Within mean-field theory, the average number \bar{n} of photons in the cavity satisfies

$$\bar{n} = \frac{2\lambda - \kappa_1}{2\kappa_2}. \quad (S3)$$

This suggests that, in the limit of $\lambda/\kappa_2 \gg 1$, the steady state of the system should start to converge to a coherent state $|\pm\mu\rangle$ with a shifted amplitude:

$$a|\pm\mu\rangle = \pm\mu|\pm\mu\rangle, \quad \mu = \sqrt{\frac{2\lambda - \kappa_1}{2\kappa_2}}e^{-i\pi/4}. \quad (S4)$$

Numerics suggest that the true steady state of the system will be a mixture of several pure states [39]. However, the steady state will have large overlap with the states $|\pm\mu\rangle$. In the limit $\kappa_1/\kappa_2 \ll 1$, the steady state will start to converge to a mixture of the states $|\pm\mu\rangle$.

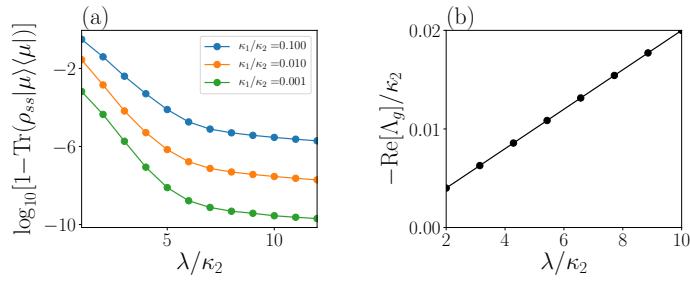


FIG. S1. Model 1: (a) Expectation value of $|\mu\rangle\langle\mu|$ in the steady state of the model described in Eqs. (S1), (S2) with $\lambda/\kappa_2 = N$ for different choices of κ_1/κ_2 . In the limit $\lambda/\kappa_2 \gg 1, \kappa_1/\kappa_2 \ll 1$, the system converges to the coherent state $|\mu\rangle$. We use exact Lindblad evolution starting from the initial state $|\alpha\rangle$ and evolving for a time $t = 200/\kappa_2$ to reach the steady state. (b) The dissipative gap Λ_g scales linearly as a function of the drive strength, for $\kappa_1/\kappa_2 = 10^{-3}$.

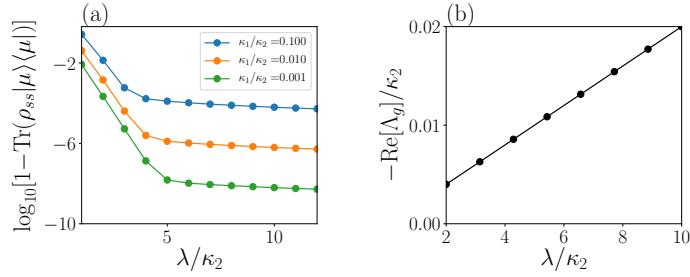


FIG. S2. Model 2: (a) Expectation value of $|\mu\rangle\langle\mu|$ in the steady state of the model described in Eqs. (S6), (S7) with parameters: $\lambda/\kappa_2 = N$ for different choices of κ_1/κ_2 . In the limit, $\lambda/\kappa_2 \gg 1, \kappa_1/\kappa_2 \ll 1$ the system converges to the coherent state $|\mu\rangle$. We use exact Lindblad evolution starting from the initial state $|\alpha\rangle$ and evolving for a time $t = 200/\kappa_2$ to reach the steady state. (b) The dissipative gap Λ_g scales linearly as a function of the drive strength, for $\kappa_1/\kappa_2 = 10^{-3}$.

We can confirm this via numerical simulations. In Fig. S1 we plot the overlap of the steady state with $|\mu\rangle$ as a function of the drive strength λ/κ_2 , for different choices of κ_1/κ_2 . We find that the steady state of the system approaches $|\mu\rangle$ in the limit $\lambda/\kappa_2 \gg 1, \kappa_1/\kappa_2 \ll 1$. These parameters are in a regime that is relevant for modern experiments [42]. We also plot the dissipative gap, which scales linearly with the drive strength.

Beyond a shift in the coherent state amplitude, single-photon loss also has the effect of reducing the qubit-steady-state structure to a classical-bit-steady-state structure. Only classical mixtures of coherent states are stable, while off-diagonal coherences have a finite lifetime:

$$\rho_{ss} \approx c|\mu\rangle\langle\mu| + (1-c)|-\mu\rangle\langle-\mu|. \quad (S5)$$

for $c \in [0, 1], \lambda/\kappa_2 \gg 1, \kappa_1/\kappa_2 \ll 1$. The steady state is thus two dimensional, enough only to store a classical bit.

Model 2: Let us now consider a different model which will have the same steady state and dissipative gap in the limit $\lambda/\kappa_2 \gg 1, \kappa_1/\kappa_2 \ll 1$, but will involve the “idealized bit flip” rather than single-photon loss. Consider the dissipators

$$L_c = \sqrt{\kappa_2}(a^2 - \alpha^2), \quad \alpha = \sqrt{\frac{\lambda}{\kappa_2}}e^{-i\pi/4} \quad (S6)$$

$$E_1 = \sqrt{\kappa_1}b = \sqrt{\kappa_1}aV, \quad V = |\alpha_e\rangle\langle\alpha_e| + |\alpha_o\rangle\langle\alpha_o| \quad (S7)$$

where $|\alpha_e\rangle \sim |\alpha\rangle + |-\alpha\rangle$, $|\alpha_o\rangle \sim |\alpha\rangle - |-\alpha\rangle$. In this model, the dissipator E_1 does not cause any leakage of photons out of $|\alpha\rangle$. This is because the non-Hermitian Hamiltonian term proportional to $E_1^\dagger E_1$ keeps superpositions of $|\pm\alpha\rangle$ in this subspace (due to the projector V). Nevertheless, the term E_1 ensures that quantum superpositions of $|\pm\alpha\rangle$ are unstable, while classical mixtures are stable. The steady state starts to converge to the following state in the limit of large drive $\lambda/\kappa_2 \gg 1$:

$$\rho_{ss} \approx c|\alpha\rangle\langle\alpha| + (1-c)|-\alpha\rangle\langle-\alpha|, \quad (S8)$$

for $c \in [0, 1]$.

The overlap between $|\alpha\rangle$ and $|\mu\rangle$ satisfies

$$|\langle\alpha|\mu\rangle|^2 = \exp\left[-\frac{\kappa_1^2}{16\kappa_2\lambda}\right] \approx 1 - \frac{\kappa_1^2}{16\kappa_2\lambda} + \dots \quad (\text{S9})$$

This implies that the deviation from unity scales as κ_1^2 when $\kappa_2\lambda \gg \kappa_1^2$. We confirm this in Fig. S2: The deviation between the steady state of Model 2 and $|\mu\rangle$ scales quadratically with κ_1 in the limit of large drive. We also plot the dissipative gap, which again scales linearly with the drive strength.

We have shown that Models 1 and 2 converge to each other in terms of their steady state and their dissipative gap in the limit $\lambda/\kappa_2 \gg 1, \kappa_1/\kappa_2 \ll 1$. This suggests that Model 2 is a reasonable approximation for Model 1 in this regime. Intuitively, this happens because the system quickly evolves toward the codespace, such that the projector term V acts trivially on the state. In the main text, we demonstrated that Model 2 passively corrects against bit flip errors via the Ising-like dissipators described above. We expect Model 1 to behave in qualitatively the same manner after the replacement of $b \rightarrow a$.

We note that, although we used the limit $\lambda/\kappa_2 \gg 1, \kappa_1/\kappa_2 \ll 1$ to establish the exact mapping to the Ising model, we do not expect that this limit is needed to preserve quantum information in general. Rather, the system only needs to stay within the ordered phase (see Fig. 3 in the main text and SM Sec. 3). A relatively small κ_1 ensures that the steady state of the dynamics is a mixed state. Nevertheless, we expect that this mixed state will be a “noiseless subsystem” [see Eq. (9) in the main text], which implies that it can be decoded with a channel superoperator at the end of the dynamics.

2. TOY MODEL

The Ising-inspired bit-flip recovery jump operators [Eqs. (11) in the main text] by themselves will not give rise to protection against single-photon loss in the absence of a drive, since single-photon loss will cause the system to evolve to a vacuum state. In this section, we argue that, when the bit-flip recovery is coupled with the driving, the resulting environment is able to protect against both dephasing and single-photon loss errors.

Ideally, we would like to numerically simulate the 2D array of M^2 cat qubits introduced in the main text. However, such a simulation is computationally expensive. We restrict ourselves to the toy model introduced in the main text: a single cat qubit coupled to a two-level system, the latter described by Pauli operators X, Y, Z . The logical states of this toy system are defined as $|\downarrow\rangle|\alpha_o\rangle$ and $|\downarrow\rangle|\alpha_e\rangle$, where $|\alpha_e\rangle, |\alpha_o\rangle$ are the logical states for a single cat qubit. The noise and recovery jump operators are modified to

$$l_c = \sqrt{\kappa_2}(a^2 - \alpha^2), \quad \alpha = \sqrt{\frac{\lambda}{\kappa_2}}e^{-i\pi/4} \quad (\text{S10})$$

$$l_1 = \sqrt{\kappa_1}Xa, \quad l_d = \sqrt{\kappa_d}a^\dagger a, \quad (\text{S11})$$

$$l_{nn} = \sqrt{\kappa_{nn}}\frac{1}{2}X(1-Z)a, \quad (\text{S12})$$

where l_c generates a Lindbladian that is equivalent to the combined action of h and l_2 in the main text. In this toy model, the spin-1/2 particle is essentially a “classical bit” that takes the discrete value of up or down. Any single-photon loss event is always accompanied by a flip of the spin. A bit-flip recovery for the cat qubit can then be achieved by checking the orientation of the spin: an annihilation operator a is applied to the cavity if the spin points upwards, otherwise nothing happens. This mimics the full 2D case where a bit-flip recovery jump is triggered by a parity misalignment between nearest-neighbor cat qubits. The difference between the 2D model and the toy model is that the latter always knows when an odd number of single photon-loss events has occurred. What remains to be tested is whether the errors can be corrected by introducing the bit-flip recovery jump.

Suppose we initialize the dynamics with a generic state in the codespace. We consider the following two scenarios: We choose the model with (i) $\kappa_2 = 1, \kappa_d = 0.1, \kappa_1 = 0.1, \kappa_{nn} = 0$ and (ii) $\kappa_2 = 1, \kappa_d = 0.1, \kappa_1 = 0.1, \kappa_{nn} = 0.3$. The system size parameter is $N = \lambda/\kappa_2$ with $N \rightarrow \infty$ representing the thermodynamic limit. The initial state is first evolved with this Lindbladian for duration $T = 15$, then followed by the corresponding noiseless Lindbladian evolution ($\kappa_d = \kappa_1 = 0$) for another $T = 15$. In the end, we compute the fidelity between the final state and the initial state. The results for the two scenarios are shown in Fig. S3 for different N .

The results clearly show distinct behaviors. For case (i), where $\kappa_{nn} = 0$, the single-photon loss causes uncorrectable errors in the stored memory, leading to a saturated fidelity of 1/2 (due to an equal mixture of the flipped and unflipped

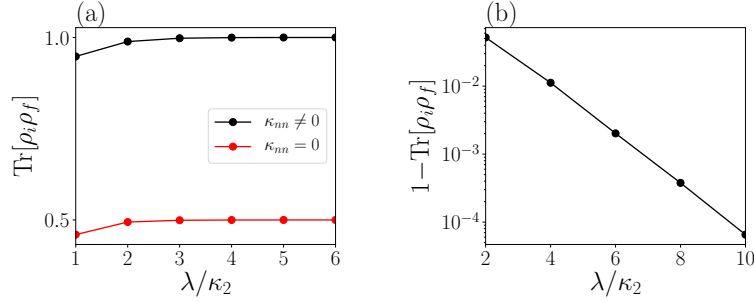


FIG. S3. We initialize the dynamics with state $\rho_i = |\psi\rangle\langle\psi|$, where $|\psi\rangle = \frac{1}{\sqrt{5}}|\downarrow\rangle|\alpha_e\rangle + \frac{2e^{i\pi/4}}{\sqrt{5}}|\downarrow\rangle|\alpha_o\rangle$. (a) Overlap between the initial and final states for $\kappa_{nn} = 0$ [case (i)] and $\kappa_{nn}/\kappa_2 = 0.3$ [case (ii)] as $N = \lambda/\kappa_2$ increases. Parameters: $\kappa_d/\kappa_2 = 0.1$, $\kappa_1/\kappa_2 = 0.1$. (b) For case (ii), i.e. $\kappa_{nn} \neq 0$, the log scale plot shows that the fidelity converges exponentially quickly to 1 as $N \rightarrow \infty$.

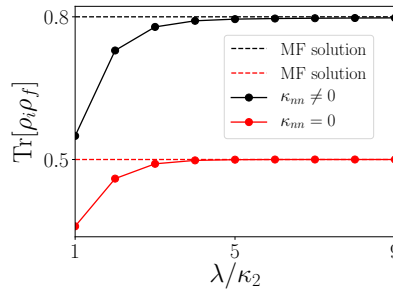


FIG. S4. Repeating the same simulation as in Fig. S3, except the recovery (noiseless) Lindblad evolution is done using $\kappa_{nn} = \kappa_d = \kappa_1 = 0$ in both cases (i) and (ii) [not just case (i)]. The overlap between the initial and final states is larger than 1/2 when $\kappa_{nn} \neq 0$ during the noisy dynamics [modified case (ii)], while the overlap saturates to 1/2 when $\kappa_{nn} = 0$ [the original case (i)]. In the thermodynamic limit, the overlap values agree with mean-field results (shown as horizontal dashed lines).

states) as N increases. For case (ii), where $\kappa_{nn} \neq 0$, increasing N leads to a fidelity exponentially close to the ideal value of 1.

As a sanity check, let us consider the same numerical simulation but modify case (ii) by setting $\kappa_{nn} = 0$ during the noiseless dynamics (while still keeping $\kappa_{nn} = 0.3$ during the noisy dynamics). The results of the simulation are shown in Fig. S4. In case (i), which is identical to the one studied in Fig. S3, the fidelity relaxes to 1/2 regardless of the system size as before. The modified case (ii) shows a saturated fidelity between 1/2 and 1, suggesting a partial preservation of the initial quantum memory. This again confirms the dynamical quantum memory protection arising from the flip-recovery jump and two-photon drive.

Mean-field analysis of the toy model.—We use a mean field approach to show that, despite the spin-boson coupling in our toy model, the \mathbb{Z}_2 symmetry-breaking phase diagram of the single cat qubit is reproduced. Given an observable \hat{O} and a Lindbladian term \mathcal{L} generated by the jump operator L , the expectation value obeys

$$\text{Tr}[\hat{O}\mathcal{L}\rho] = -\frac{1}{2}\text{Tr}\left[[\hat{O}, L^\dagger]L\rho + L^\dagger[L, \hat{O}]\rho\right]. \quad (\text{S13})$$

Using this, we can derive a coupled set of mean-field equations of motion for $\langle a \rangle$ and $\langle Z \rangle$:

$$\frac{d}{dt}\langle a \rangle = -i\lambda\langle a^\dagger \rangle - \frac{1}{2}\left(\kappa_1 + \kappa_d + \frac{\kappa_{nn}}{2}(1 - \langle Z \rangle)\right)\langle a \rangle - \kappa_2|\alpha|^2\langle a \rangle, \quad (\text{S14})$$

$$\frac{d}{dt}\langle Z \rangle = -2\kappa_1|\alpha|^2\langle Z \rangle + \kappa_{nn}|\alpha|^2(1 - \langle Z \rangle). \quad (\text{S15})$$

This yields the mean-field fixed point solutions for both observables

$$\langle Z \rangle = \frac{\kappa_{nn}}{\kappa_{nn} + 2\kappa_1}, \quad (\text{S16})$$

$$\kappa_2|\alpha|^2 = |\lambda| - \frac{1}{2}\left(\kappa_1 + \kappa_d + \frac{\kappa_1\kappa_{nn}}{\kappa_{nn} + 2\kappa_1}\right). \quad (\text{S17})$$

The expression closely matches the simulation in the thermodynamic limit (see Fig. S4).

It is interesting to note that if κ_1/κ_2 is small enough, then any non-zero κ_{nn} can give rise to a stable memory ($\langle Z \rangle, \langle a \rangle \neq 0$). On the other hand, if κ_1/κ_2 is large, a large κ_{nn} can destabilize the memory, leading to $\langle a \rangle = 0$.

3. MEAN-FIELD SOLUTION FOR THE 2D PHOTONIC-ISING MODEL

In this section, we present the mean-field solution for the 2D photonic-Ising model. The mean-field analysis shows the existence of two symmetry-breaking transitions via two order parameters: a^2 and $Q \equiv e^{i\pi a^\dagger a}$.

We consider a product-state mean-field ansatz $\rho = \bigotimes_{x,y=1}^M \rho_{x,y}$. At each site, $\rho_{x,y}$ is a density matrix for a two-level system in the basis of $|\pm\alpha_{MF}\rangle$ for some coherent parameter α_{MF} . We first begin by deriving the mean-field equation for $Q = e^{i\pi a^\dagger a}$. Note that all the terms that commute with Q do not contribute to the time evolution. We are therefore left to consider only the single-photon loss term and the bit-flip correction term. Using Eq. (S13), we obtain

$$\frac{d\langle Q \rangle}{dt} = -2 (\kappa_1 \langle a^\dagger a Q \rangle + \kappa_{nn} \langle a^\dagger a Q P_{\kappa_{nn}} \rangle + \tilde{\kappa}_{nn} \langle a^\dagger a Q P_{\tilde{\kappa}_{nn}} \rangle), \quad (\text{S18})$$

where $P_{\kappa_{nn}}, P_{\tilde{\kappa}_{nn}}$ are sums of projectors onto different parity configurations with rates $\kappa_{nn}, \tilde{\kappa}_{nn}$, as introduced in the main text. Within mean-field theory, we replace the expectations by a product of expectations at each site, yielding

$$-\frac{1}{2|\alpha|^2} \frac{d\langle Q \rangle}{dt} = \frac{\kappa_{nn} - 4\tilde{\kappa}_{nn}}{16} \langle Q \rangle^5 + \frac{\kappa_{nn} + 4\tilde{\kappa}_{nn}}{8} \langle Q \rangle^3 - \left(\frac{3\kappa_{nn} + 4\tilde{\kappa}_{nn}}{16} - \kappa_1 \right) \langle Q \rangle. \quad (\text{S19})$$

Similarly, we can derive the mean-field equation for a^2 :

$$\frac{d\langle a^2 \rangle}{dt} = -\kappa_2 (2\langle a^\dagger a a^2 \rangle + \langle a^2 \rangle) - i\lambda (2\langle a^\dagger a \rangle + 1) - \kappa_1 \langle a^2 \rangle - 2\kappa_d \langle a^2 \rangle - \kappa_{nn} \langle a^2 P_{\kappa_{nn}} \rangle - \tilde{\kappa}_{nn} \langle a^2 P_{\tilde{\kappa}_{nn}} \rangle. \quad (\text{S20})$$

With the mean-field ansatz, we may approximate $\langle a^\dagger a a^2 \rangle \approx |\alpha_{MF}|^2 \langle a^2 \rangle$. We also have $\langle a^2 P_{\tilde{\kappa}_{nn}} \rangle = \langle a^2 \rangle \langle P_{\tilde{\kappa}_{nn}} \rangle$ and $\langle a^2 P_{\kappa_{nn}} \rangle = \langle a^2 \rangle \langle P_{\kappa_{nn}} \rangle$. After some algebra, the mean-field fixed points at the thermodynamic limit (e.g. $\kappa_2 \rightarrow 0$) can be found to satisfy

$$\langle Q \rangle^2 = \frac{2\sqrt{\kappa_{nn}^2 - 4\kappa_1(\kappa_{nn} - 4\tilde{\kappa}_{nn})} - \kappa_{nn} - 4\tilde{\kappa}_{nn}}{\kappa_{nn} - 4\tilde{\kappa}_{nn}}, \quad (\text{S21})$$

$$|\alpha_{MF}|^2 = \frac{2\lambda - \kappa_1 - 2\kappa_d - \gamma_4 \langle Q \rangle^4 - \gamma_2 \langle Q \rangle^2 - \gamma_0}{2\kappa_2}, \quad (\text{S22})$$

where $\gamma_4 = (-3\kappa_{nn} + 4\tilde{\kappa}_{nn})/16$, $\gamma_2 = (\kappa_{nn} - 4\tilde{\kappa}_{nn})/8$, and $\gamma_0 = (\kappa_{nn} + 4\tilde{\kappa}_{nn})/16$. In addition, $\langle Q \rangle^2 \neq 0$ is only possible when $|\alpha_{MF}|^2 \neq 0$. Intuitively, when $\langle a^2 \rangle = 0$, the cavity will lose coherence and decay to the vacuum due to the noise. The logical states are no longer well-defined in this case.

It is important to note that the mean-field solution suggests that the leakage caused by both finite κ_1 and finite κ_d is compensated by the two-photon drive. The effect of this leakage amounts to a shift in the steady state coherent parameter.